Incommensurate versus Commensurate Description of the A_xBX_3 Hexagonal Perovskite-Type Structure. $Sr_{1.2872}NiO_3$ Incommensurate Composite Compound Example

M. Evain,* F. Boucher, and O. Gourdon

Laboratoire de Chimie des Solides, IMN, UMR C6502 CNRS, Université de Nantes, 2 Rue de la Houssinière, BP 32229, 44322 Nantes Cedex 3, France

V. Petricek and M. Dusek

Institute of Physics, Academy of Sciences of the Czech Republic, Na Slovance 2, 180 40 Praha 8, Czech Republic

P. Bezdicka

Institute of Inorganic Chemistry, Academy of Sciences of the Czech Republic, Pelléova 24, 160 00 Praha, Czech Republic

Received March 24, 1998. Revised Manuscript Received June 4, 1998

We report a new structure determination of the $Sr_{1.2872}NiO_3$ incommensurate composite hexagonal perovskite compound. Three different refinement strategies are presented: (i) a 3D supercell approximation with a nonharmonic development of the atomic displacement factor, (ii) an original (3+1)D incommensurate composite description with the use of crenel functions, and (iii) a (3+1)D commensurate composite model. The three strategies are discussed and compared to previous refinements carried out for the hexagonal perovskites in a classical way or with the superspace group formalism. Out of the three methods, the incommensurate composite approach gives slightly better results with a final global R value of 2.89% for 635 independent reflections (at a $I/\sigma(I) > 2$ level) and only 60 parameters ($R\bar{3}m(00\gamma)0$s superspace group; $a = 9.5177(7)$ Å, $c = 2.5739(2)$ Å, $\mathbf{q} = 0.64359(4)\mathbf{c}^*$, $V = 201.93(4)$ Å^3, and $Z = 3$). The use of crenel functions notably improves previously reported results. New structural features are evidenced for $Sr_{1.2872}NiO_3$: (i) an incommensurate character, (ii) a splitting of the trigonal prismatic nickel atoms over 5 positions, (iii) a definite stoichiometry which induces a perfect charge balance, and (iv) a nonharmonic behavior of some Sr atoms. Those characteristics seem general to most hexagonal perovskite compounds and essential for correctly interpreting their interesting magnetic properties. Finally, a new generic formulation is proposed, which explains the various stoichiometries observed and suggests a new compound possibility.

1. Introduction

The A_xBX_3 hexagonal perovskite-type compounds, up to now usually generically formulated as $A_{3n+3}A'_nB_{n+3}X_{6n+9}$, have recently received a particular attention. Indeed, for some A′/B combinations (e.g. Ir/Ni or Cu/(Pt,Ir)) interesting magnetic properties have been observed, such as complex magnetism[1] or random spin chain magnetism.[2] The structures are built up from infinite $[BX_3]$ chains consisting of alternating octahedral and trigonal prismatic units, separated by A_∞ chains. Structural relationships with the usual perovskites have been formulated in terms of stacking of mixed $[A_3X_9]$ and $[A_3A'X_6]$ layers.[3,4]

However, many structures of hexagonal perovskite-type compounds are not yet fully characterized, either because of a lack of single crystals or, when single crystals are available, because of a reduced data set and/or an inappropriate data treatment. In addition, no uniform structural analysis has been used so far, a commensurate supercell approach being most of the time preferred, but an incommensurate composite crystal description being sometimes chosen.[5,6] Consequently, for clear interpretations of the magnetic properties, crucial questions need to be answered. First, is the A′ nonstoichiometry sometimes reported genuine or

* To whom correspondence should be addressed.

(1) Nguyen, T. N.; zur Loye, H.-C. *J. Solid State Chem.* **1995**, *117*, 300.
(2) Nguyen, T. N.; Lee, P. A.; zur Loye, H.-C. *Science* **1996**, *271*, 489.
(3) Darriet, J.; Subramanian, M. A. *J. Mater. Chem.* **1995**, *5*, 543.
(4) Dussarrat, C.; Grasset, F.; Darriet, J. *Eur. J. Solid State Inorg. Chem.* **1995**, *32*, 557.
(5) Ukei, K.; Yamamoto, A.; Watanabe, Y.; Shishido, T.; Fukuda, T. *Acta Crystallogr.* **1993**, *B49*, 67.
(6) Onoda, M.; Saeki, M.; Yamamoto, A.; Kato, K. *Acta Crystallogr.* **1993**, *B49*, 929.

10.1021/cm9801800 CCC: $15.00
Published on Web 09/25/1998

simply due to an inappropriate structure description? For example, $Sr_{12}Ni_{7.5}O_{27}$ and $Sr_9Ni_{6.64}O_{21}$ are announced as significantly different from their ideal stoichiometric counterparts $Sr_{12}Ni_9O_{27}$ and $Sr_9Ni_7O_{21}$, respectively.[7,8] Second, is the A′ cation located on the trigonal prismatic 3-fold axis or displaced from this axis toward the prism faces? In most structure refinements reported in the literature, the A′ cation is placed on the axis, although hints such as very large atomic anisotropic displacement parameters (ADP) suggest a displacement away from this axis. These typical descriptions seem related to poor data sets (single crystals) or a lack of information (powders) or an inappropriate model (superspace group approach). Notice that lowering the site occupancy generates the aforementioned nonstoichiometry but does not reduced the large ADPs. Third, are the structures commensurate or incommensurate and what is the most pertinent model for the structure description? Finally, is it possible to find various succession of octahedra and trigonal prisms for the same elements and how can the charge balance be easily established?

To answer those questions, several structures in the hexagonal perovskite-type family are presently reconsidered and new compounds characterized. In this paper, we report a thorough analysis of the $Sr_{1.2872}NiO_3$ incommensurate composite structure. We compare two structure models: (i) a classical supercell model that can be considered because of the closeness of the hypothetical commensurate $Sr_{18}(NiO_3)_{14}$ ($Sr_{1.2857}NiO_3$) counterpart and because of a high symmetry which limits the number of parameters (this model will be dramatically improved with an anharmonic development of the atomic displacement factor) and (ii) an incommensurate composite model taking into account the structure particularities by means of crenel functions (this last model will be demonstrated to be a major improvement of the classical incommensurate composite model already used for similar compounds). Finally, we analyze the structural results and propose a new scheme for a generic formulation of the hexagonal perovskite-type compounds.

2. Experimental Section

2.1. Synthesis and Characterization. $Sr_{1.2872}NiO_3$ single crystals were grown by heating, for 10 min in an alumina crucible at 1025 K, a mixture of reagent grade $SrCO_3$, NiO, and KOH in a Sr:Ni:K = 1:1:10 molar ratio. The mixture was then reheated for 10 min at 1373 K and subsequently cooled to room temperature in the furnace. The final product was recovered from the melt by washing with distilled water. Finally, the crystals were dried at 373 K.

The as prepared single crystals were examined by electron microprobe (JEOL JXA-733). They were found to be free of Al. However, they contained traces of K (≈1%). The X-ray diffractogram revealed no impurities.

2.2. Data Collection. With regard to the desired quality of the results, special care was paid to the selection of the single crystal to be used for the structure determination. A first selection of good quality crystals was first carried out with a Weissenberg camera. It should be noticed that only a minority of the original batch had the required quality for a further selection. Each selected crystal was then tested for perfection and scattering power on a Stoe image plate system (IPDS). Two crystals were finally chosen. Both crystals were subsequently fully analyzed and gave strictly identical refinement results (position, site occupancy, etc.). Since one data set had more observed reflections than the other one, we will only consider the best set in this report.

Two different data collections were initiated. A first collection was carried out on a Stoe IPDS in a medium-resolution mode (IP at 80 mm) with long exposure times to accurately measure weak reflection intensities at low $\sin(\theta)/\lambda$ values (up to 0.57). The strongest reflections were not measured in that mode because of a saturation of the image plate. A second collection was performed on a Nonius CAD-4F diffractometer to complete the data with reflections that were missed in the first collection and with additional reflections up to $\sin(\theta)/\lambda = 0.8$. Both data sets were consistent with a trigonal symmetry and could be described in an *R* centered hexagonal Bravais lattice ($a \approx 9.50$ Å, $c \approx 35{,}96$ Å). However, the misfit character of the structure with two distinct main subsets and satellite reflections was clear from the diffraction pattern. From a precise centering of 41 reflections on the CAD-4F diffractometer and with a (3 + 1) integer indexing, the refinement of the cell parameters with the U-fit program[9] led to the following lattice parameters: $a_s = 9.5177(7)$ Å, $c_s = 2.5739(2)$ Å, $\mathbf{q} = 0.64359(4)\mathbf{c^*}$, and $V_s = 201.93(4)$ Å^3. The [NiO_3] first subsystem and [Sr] second subsystem reflection sets are obtained from the (3+1)D superspace reflection indices by the $\mathbf{W}^1$ and $\mathbf{W}^2$ transformation matrices, respectively:

$$\mathbf{W}^1 = \begin{bmatrix} 1 & 0 & 0 & 0 \\ 0 & 1 & 0 & 0 \\ 0 & 0 & 1 & 0 \\ 0 & 0 & 0 & 1 \end{bmatrix} \quad \text{and} \quad \mathbf{W}^2 = \begin{bmatrix} 1 & 0 & 0 & 0 \\ 0 & 1 & 0 & 0 \\ 0 & 0 & 0 & 1 \\ 0 & 0 & 1 & 0 \end{bmatrix}$$

(for a complete description of the concepts and the notations used for incommensurate composite structures, see for instance ref 10 and references cited therein). In this incommensurate composite description, the γ component of the modulation vector is close, but significantly different from the $9/14 \approx 0.64286$ rational ratio (difference $> 18\sigma(\gamma)$ and a much better least squares refinement: $R = 0.3\%$ instead of $R = 0.9\%$). Therefore the structure should a priori be considered as incommensurate, an assumption later on confirmed by the refinements (vide infra). The simplest supercell that can be considered is the cell used for the data collection, that is the cell corresponding to $a = 9.524(2)$ Å, $c = 36.008(5)$ Å (i.e. $\approx 14c_s$), and $V = 2828.5(13)$ Å^3. For data collection details, see Table 1.

2.3. Data Processing. Data reduction, absorption corrections, and all refinements were carried out with a β version of the JANA98 program package.[11] Measured intensities were corrected for scale variation based upon standards (CAD4 data set only) and Lorentz and polarization effects (CAD4 and IPDS sets). Prior to a Gaussian-type analytical absorption correction, an optimization of the crystal size based upon ψ-scan measurements was performed with the X-shape program.[12]

3D Option. Both data sets (IPDS and CAD4) were merged on a common scale established from mutual reflections with $I \geqslant 10\sigma(I)$, leading to a 13 792 reflection set. Those reflections were then merged according to $\bar{3}m$ point group, with an internal *R* (obs) value of 3.2% and a $I/2\sigma(I)$ cutoff as a criterion for observed reflections. Out of the 1378 independent reflections, 635 observed reflections were used in subsequent refinements. A quick analysis of the extinction rules indicated $R\bar{3}c$ and $R3c$ as possible space groups.

(7) Campa, J.; Gutierrez-Puebla, E.; Monge, A.; Rasines, I.; Ruiz-Valero, C. *J. Solid State Chem.* **1994**, *108*, 230.
(8) Campa, J.; Gutierrez-Puebla, E.; Monge, A.; Rasines, I.; Ruiz-Valero, C. *J. Solid State Chem.* **1996**, *126*, 27.
(9) Evain, M. *U-fit*: *A cell parameter refinement program*; Institut des Matériaux: Nantes, France, 1992.
(10) van Smaalen, S. *Crystallogr. Rev.* **1995**, *4*, 79.
(11) Petricek, V.; Dusek, M. *JANA98*: *Programs for modulated and composite crystals*; Institute of Physics: Praha, Czech Republic, 1998.
(12) *Stoe X-Shape*: *Crystal optimisation for numerical absorption correction*; Stoe & Cie GmbH: Darmstadt, Germany, 1996.

Table 1. Crystallographic Data for $Sr_{1.2872}NiO_3$

(a) Physical, Crystallographic, and Analytical Data

	3D option	(3+1)D option
formula	$Sr_9Ni_7O_{21}$	$Sr_{1.2872}NiO_3$
cryst color	black	
MW ($g \cdot mol^{-1}$)	1535.4	219.34
cryst syst	trigonal	
space group	$R\bar{3}c$	$R\bar{3}m(00\gamma)0s$
temp (K)	293	
cell params (from 41 reflecns centered on CAD4)		
a (Å)	9.524(2)	9.5177(7)
c (Å)	36.008(5)	2.5739(2)
		$\mathbf{q} = 0.64359(4)\mathbf{c}^*$
V (Å^3)	2828.5(13)	201.93(4)
Z	6	3
dens (calc, $g \cdot cm^{-3}$)	5.406	5.412
cryst description	needle	
cryst size (mm^3)	$\sim 0.19 \times 0.03 \times 0.02$	

(b) Data Collection

	Enraf−Nonius CAD-4F	Stoe IPDS
monochromator	oriented graphite (002)	
radiation	Mo K $L_{2,3}$ ($\lambda = 0.710\ 73$ Å)	
scan mode	$\omega/2\theta$	ω
no. of measured reflecns	9256	6504
hkl range	$-15 < h < 0$	$-11 < h < 12$
	$-13 < k < 15$	$-12 < k < 12$
	$-57 < l < 57$	$-43 < l < 45$
$\sin(\theta)/\lambda$ range	0−0.8	0−0.57
no. of std reflecns	3	na
freq of std reflecns (s)	3600s	na

(c) Data Reduction

	Enraf−Nonius CAD-4F	Stoe IPDS
linear absorpn coeff (cm^{-1})	324.9	
absorpn correcn	analytical	
T_{min}/T_{max}	0.14/0.28	0.09/0.28
scaling selection criterion	$I > 10\sigma(I)$	
scaling coeff (CAD4/IPDS)	0.7335(10)	
no. of reflecns	13792	
no. of independent reflecns	1378	
criterion for obsd reflecns	$I > 2\sigma(I)$	
R_{int} (obsd)	0.032	
no. of obsd reflecns	635	

(d) Refinement

	supercell	incommensurate
refinement	F	
$F(000)$	4236	303
no. of reflecns used in the refinement	635	
R^a (%)	2.92	2.89
$R_w{}^a$ (%)	3.09	2.87
S	1.80	1.66
no. of refined params	69	60
weighting scheme	$w = 1/(\sigma^2\|F_o\|+(0.02)\|F_o\|)^2)$	
diff Fourier residues	[−1.3,+1.2] e$^-$/Å^3	[−1.3,+1.0] e$^-$/Å^3

[a] $R = \sum||F_o| - |F_c||/\sum|F_o|$. $R_w = [\sum w(|F_o| - |F_c|)^2/\sum w|F_o|^2]^{1/2}$.

(3+1)D Option. Prior to averaging, each Fourier wave vector was indexed with four indices in the M^* vector module of rank 4. An additional transformation had to be performed to keep an obverse setting (the initial obverse setting is indeed transformed to a reverse setting in the course of the 3D → (3+1)D transformation). The aforementioned procedure was then carried out for the merging of the two data sets and the averaging according to the $(\bar{3}m,\bar{1}1)$ point group. Obviously, with the same conditions, the same number of independent observed reflections was obtained. Combined with the $h-k-l = 3n$ general condition, the $hhlm$:$m = 2n$ special reflection condition suggested two possible trigonal superspace groups: $R\bar{3}m(00\gamma)0s$ and $R3m(00\gamma)0s$, centrosymmetric and non-centrosymmetric, respectively. For data processing details, see Table 1.

Table 2. Fractional Atomic Coordinates and Equivalent Isotropic Displacement Parameters[a] (Å^2) for $Sr_{1.2872}NiO_3$ (3D Option)

	x	y	z	B_{eq}	τ
Sr1	0.6842(3)	0.0205(2)	0.02772(6)	1.10(3)	
Sr2	0.3237(4)	0	3/4	1.46(4)	
Ni1	0	0	0	1.28(9)	
Ni2	0	0	0.06987(11)	1.51(7)	
Ni3a	0.0023(4)	0.0636(3)	0.1411(2)	0.39(3)[b]	0.561(4)
Ni3b	0	0	0.1510(4)	0.39(3)[b]	0.275(3)
Ni3b′	0	0	0.1379(3)	0.39(3)[b]	0.164
Ni4	0	0	0.21596(7)	0.18(5)	
O1	0.1530(7)	0.1522(7)	0.0988(2)	2.4(2)	
O2	0.1655(10)	0.1577(10)	0.1848(3)	2.7(2)	
O3	0.1486(9)	0.1579(9)	0.5330(16)	0.32(10)[b]	
O4	0.1546(12)	0.1546	3/4	1.3(2)	

[a] $B_{eq} = (8\pi^2/3)\sum_i\sum_j U^{ij}a_i^*a_j^*\mathbf{a}_i\mathbf{a}_j$. [b] B_{iso}.

2.4. Refinements. *3D Option*. Starting with the model proposed by Campa et al.,[8] the refinement smoothly converged to a solution with a residual R value of 7.7% for independent ADPs. As indicated by Campa et al., the Ni3 atom in the trigonal prismatic site presented huge U^{11} and U^{22} values. However, freeing the site occupancy did not improve the results, and the Ni3 population factor remained around the unity. Difference Fourier maps revealed strong residues (ca. 11 e$^-$/Å^3) in the three rectangular faces of the trigonal prism. Displacing the Ni3 atom from the chain 3-fold axis conclusively improved the residue factor ($R = 4.7\%$). A new difference Fourier map series then revealed two important peaks on the axis, above and below the center of the trigonal prism. Several split models were then attempted, the best one corresponding to three independent positions: a position (Ni3a) away from the axis (yielding a fractional occupancy of the prism faces) and two positions (Ni3b and Ni3b′) on the 3-fold axis, on both sides of the trigonal prism center. With the Ni3 positions being separated by rather short distances (ca. 0.5 Å), a unique isotropic displacement parameter was used. Refinements of this model led to a residual factor of 3.96% for 59 parameters.

The residues calculated at this stage of the refinement, ca. 2.2 e$^-$/Å^3, were located in the vicinity of Sr1. Among the two independent strontium atoms, Sr1 is closer to the Ni3 split atoms; it is therefore the most affected by the disorder, and its ADPs should deviate from harmonic terms (for a generalized description of the atomic displacement in crystallographic structure analysis, see for instance ref 13 and references cited therein). The introduction of Gram−Charlier third-order tensor coefficients in the development of the Sr1 atomic factor considerably improved the results. A 1% drop of the residual factor ($R = 2.92\%$ and $R_w = 3.09$ for 69 variables) was indeed observed, and the difference Fourier map residues were considerably reduced. In addition the C^{ijk} coefficients were highly significant, and the Sr1 probability density function was free from important negative regions. A similar description of Sr2 with higher order terms had no effect. Final refined atomic site parameters obtained for the 3D option are gathered in Table 2.

Incommensurate (3+1)D Option. In a composite structure, each subsystem μ is modulated by the other subsystems. In $Sr_{1.2872}NiO_3$, there are two subsystems and each subsystem has a one-dimensionally modulated structure, the modulation period of one subsystem occurring as the c^*_μ basic period of the other subsystem. A classical refinement of such a composite structure proceeds as follows. The average structure is classically determined from the main reflections. Then displacive and/or occupational modulations are introduced by means of Fourier series expansions. Debye−Waller factor (DWF) modulations can also be considered.

For the title compound, the structure refinement was initiated with a structural model similar to that proposed by

(13) Kuhs, W. F. *Acta Crystallogr. A* **1992**, *48*, 80.

Ukei et al. for $Ba_{1.317}(Pt,Cu)O_3$,[5] that is, in the $R\bar{3}m(00\gamma)0s$ non-centrosymmetric superspace group with three independent positions (Ni1 at (0,0,0), Sr at ($^1/_3$,0,0) and O at ($2x$,x,$^1/_2$), $x \approx 0.07$). The R residual factor smoothly converged to a value of ca. 8.5% upon addition of successive displacive Fourier amplitude waves (fourth order for Sr and Ni1 and sixth order for O) and DWF waves (fourth order for Sr and Ni1). DWF modulations had to be introduced in the calculation because of the various sites occupied by the nickel atoms and the disordered character of the structure (vide infra). Although 62 parameters were already introduced in the calculation, the F_{obs}/F_{calc} agreement was not satisfactory (but of the order of that of Ukei et al. for $Ba_{1.317}(Pt,Cu)O_3$), and large residues were observed in the difference Fourier maps around the nickel atoms in the trigonal prismatic sites, away from the 3-fold axis. Several possibilities of displacing the Ni1 atom from the axis were then considered. They all resulted in an important lowering of the residual factor (the R could reach a value as low as 2.65% for Ni1 in a general position) but with far too many parameters (up to 72) and, more importantly, with nonphysical Ni1−O distances. A new model was then developed.

In Ukei's model, the oxygen atom is placed on the ($m_x1|0,0,0,^1/_2$) symmetry element at $z = {}^1/_2$ as shown in **1**.

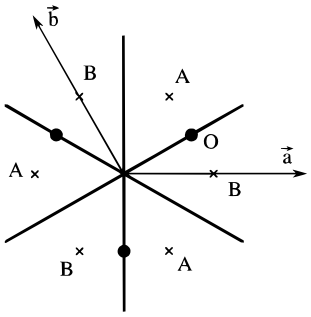

1

However, via the displacive modulations, O is never found on the mirror element, but either on one side (A position) or on the other side (B position) of that element. In fact the modulation is very close to a step function, which explains the necessity of high-order displacive waves. Another description of the structure is therefore possible. Using the $R\bar{3}m(00\gamma)0s$ centrosymmetric superspace group, the oxygen atom can be located, for instance, on the A position at $z = {}^1/_2$. Through the symmetry operations six positions are then generated in the same plane (three A and three B positions). A model equivalent to that obtained in the non-centrosymmetric space group is thus achieved by modulating the O population. Once again, high-order waves are necessary to obtain a crenel-like function that exclusively splits the oxygen positions in either A or B sets.

A better way to model those two sets of well-defined positions is to use a built-in crenel function for the oxygen occupation modulation.[14,15] This is preferable in many respects. First, it dramatically reduces the number of parameters. Indeed, only two parameters are required to describe an occupation crenel function for an atom ν: the crenel width (Δ^ν) and the crenel midpoint ($\hat{x}_4^\nu$). Second, it avoids nonphysical occupation probabilities inherent to the use of a limited number of harmonic functions in the Fourier series expansion. Finally, it prevents intermediate states produced by the Fourier series expansion at the crenel-like "steps" (in the present case, the simultaneous presence of A and B positions). Such a procedure was initiated.

(14) Petricek, V.; van de Lee, A.; Evain, M. *Acta Crystallogr. A* **1995**, *51*, 529.
(15) Boucher, F.; Evain, M.; Petricek, V. *Acta Crystallogr. B* **1996**, *52*, 100.

Table 3. Symmetry Operations of the $R\bar{3}m(00\gamma)0s$ Superspace Group

(1) (E 1|n_1 n_2 n_3 n_4)	(7) (i $\bar{1}$|0 0 0 0)
(2) (3_z^+ 1| 0 0 0 0)	(8) ($\bar{3}_z^+$ $\bar{1}$|0 0 0 0)
(3) (3_z^- 1| 0 0 0 0)	(9) ($\bar{3}_z^-$ $\bar{1}$|0 0 0 0)
(4) (m_x 1|0 0 0 $^1/_2$)	(10) (2_x $\bar{1}$|0 0 0 $^1/_2$)
(5) (m_y 1|0 0 0 $^1/_2$)	(11) (2_y $\bar{1}$|0 0 0 $^1/_2$)
(6) (m_{xy} 1|0 0 0 $^1/_2$)	(12) (2_{xy} $\bar{1}$|0 0 0 $^1/_2$)
+ (E 1|$^1/_3$ $^2/_3$ $^2/_3$ 0)	+ (E 1|$^2/_3$ $^1/_3$ $^1/_3$ 0)

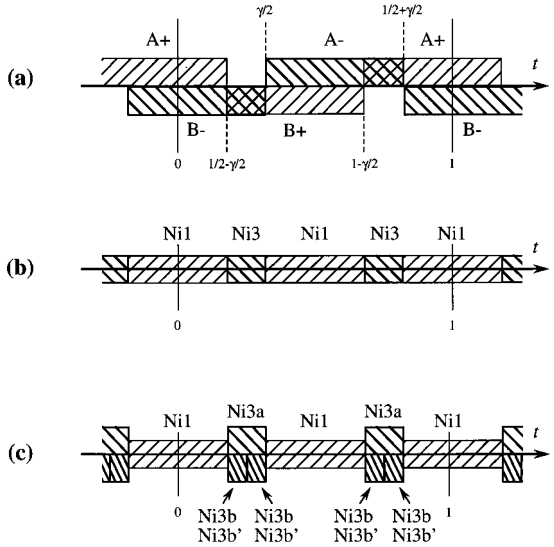

Figure 1. Domain limits of the various crenels used in the structure determination: (a) the oxygen crenels giving rise to the octahedral and trigonal prismatic sites, (b) the separation between the octahedral (Ni1) and trigonal prismatic (Ni3) nickel atoms, and (c) the splitting of the trigonal prismatic into three independent positions (Ni3a, Ni3b, and Ni3b′).

We assume that O(A) atoms are defined on a crenel of width $\Delta^{O(A)}$ centered at $\hat{x}_4^{O(A)}$. Then O(B) atoms are defined on a crenel (of same width) related by symmetry operations to the first crenel (see Table 3 for the $R\bar{3}m(00\gamma)0s$ superspace group symmetry operations). The conditions that the O atoms should be found either in the A or in the B position determine the width and the center of the crenels ($\Delta^{O(A)} = {}^1/_2$ and $\hat{x}_4^{O(A)} = {}^1/_4$). The various crenels for oxygen atoms (O(A+) for the oxygen A position at $z = +{}^1/_2$, etc.) are presented in Figure 1a. The second subsystem, i.e., the strontium atoms, should have a position compatible with that of the first subsystem. In the non-centrosymmetric superspace group and with the Fourier expansion of the occupation modulation, the Sr z coordinate was not so important since the crenel-like occupation function could shift along the internal coordinate. In the centrosymmetric superspace group, the oxygen position is determined by the crenel function and its coordinate imposed by the inversion center. Consequently, the second subsystem position has to be adapted accordingly. This adjustment corresponds to a $z = {}^1/_4$ shift of Sr, as compared to Ukei's model.

Upon successive addition of displacive Fourier amplitude waves (fourth order for Sr and Ni1 and second order for O) and DWF waves (fourth order for Sr and Ni1), that is, for only 34 variables, the refinement series of the new structure model led to an R residual factor of 9.9%. Notice that an orthogonalization procedure was necessary to reduce correlations. Indeed, with the application of crenel functions, the modulation functions are not defined for all values and thus the orthogonality condition is not fulfilled for the set of harmonic functions.[14] At that stage of the refinement, difference Fourier syntheses revealed strong positive and negative residues around Ni1 atoms with maxima at $t \approx 0.25$ and $t \approx 0.75$. To identify those nickel atoms, the Ni1 environment has to be analyzed as a function of t. Each Ni1 atom (at $z = 0$) is

surrounded by six O atoms, three atoms at $z = {}^1/_2$ (O(A+) or O(B+)) and three atoms at $z = -{}^1/_2$ (O(A−) or O(B−)). Depending upon t values, the nickel atoms will be either in trigonal prismatic sites (O(A+)/O(A−) or O(B+)/O(B−) combinations) or in octahedral sites (O(A+)/O(B−) or O(A−)/O(B+) combinations). The difference Fourier map residues are observed for $t = 0.25$ and $t = 0.75$, thus for nickel atoms in trigonal prismatic coordination (see Figure 1a). Notice that those results are similar to those obtained with Ukei's model (vide supra). Adding new waves for the Ni1 displacive modulations and/or displacing Ni1 from the axis were then attempted, but although it improved the refinements, it led to unrealistic Ni1−O distances and implied a large number of parameters. The problem lied in the fact that different nickel atoms (atoms in octahedra and in trigonal prisms) were modeled by one unique position. To solve that problem, a splitting of the Ni1 position with crenel functions was achieved.

The Ni1 atoms at (0,0,0) were restricted to the octahedral sites by means of a crenel function of width $1 - \gamma$ and centered at $t = 0$ (see Figure 1b). Notice that a second atom is generated through symmetry at $t = {}^1/_2$. The other nickel atoms, i.e., those in trigonal prismatic sites (O(A+)/O(A−) or O(B+)/O(B−) combinations), could be described by a new position, Ni3a, restricted to suitable t intervals by means of complementary occupation crenels. To take into account the observed residues around that prismatic center position (vide supra), Ni3a was introduced at (x,x,0) (with an occupation factor of ${}^1/_3$ to fulfill a total occupation of the prisms) and defined with only one crenel of width $\gamma - {}^1/_2$ and centered at $t = {}^1/_4$. This Ni3a new position was refined isotropically with a first-order displacive Fourier amplitude wave. Using orthogonalizations for O, Ni1, and Ni3a modulation functions and a secondary extinction coefficient (type I, Lorentzian distribution),[16] the residual factor smoothly converged to $R = 4.71$ ($R_w = 4.87$) for 52 parameters. If this new structure modeling can be considered as an improvement of the original description, new difference Fourier synthesis series revealed, however, important negative residues on Ni3a positions and positive residues (ca. 4 $e^-/Å^3$) on the axis, above and below Ni3a.

To explain those maxima and reduce the electron density on the Ni3a positions (in doing so preserving the trigonal site full occupancy), two new positions (Ni3b and Ni3b′) were introduced on the $\bar{3}$ axis on two independent (0,0,z) positions (with z(Ni3b) ≈ 0.1 and z(Ni3b′) ≈ −0.1). To generate independent positions, crenels twice as small as the crenel used for the Ni3a description and of multiplicity ${}^1/_6$ had to be considered (see Figure 1c). Both positions were defined using the right part of the crenels at $t = {}^1/_4$ and $t = {}^3/_4$, the left part corresponding to the definition domain of the 2-fold symmetry related (0,0,−z) positions. In practice, Ni3b et Ni3b′ were introduced at (0,0,z) with only one crenel of width $\gamma/2 - {}^1/_4$ and centered at $t = \gamma/4 + {}^1/_8$ (see Figure 1c), implying a change of the multiplicity to ${}^1/_6 \times 2 = {}^1/_3$. Those two new positions (Ni3b and Ni3b′) were not modulated and kept isotropic. In addition, the total trigonal prismatic site occupancy was constrained to a full site occupancy and the Ni3a, Ni3b, and Ni3b′ DWF's set equal. The residual factor dropped from 4.71 to 3.48% for only three additional parameters. Difference Fourier maps then indicated residues around the Sr atoms of the second subsystem. New waves were added for a better description of Sr atoms (up to the sixth order for the position and up to the fifth for the DWF) and the final residual factor set at 2.89% ($R_w = 2.87$) for only 60 parameters and 635 observed reflections. No significant peaks could then be observed in the difference Fourier syntheses. Since the release of the restraint on the trigonal prismatic site occupancy suggested a full occupancy of the site (101(3)%), the restraint was kept in the refinement. It is worth noticing that the introduction of high-order DWF' waves for Sr has effects similar to the introduction of nonharmonic Gram−Charlier terms if the 3D approach. In the current state of the Jana refinement program, it is not possible to distinguish the DWF modulation terms from the DWF nonharmonic terms. Final parameters for this incommensurate model are gathered in Tables 4−6.

Table 4. Final Residual Factors for $Sr_{1.2872}NiO_3$ (Incommensurate Option)

	N	R	R_w
main	225	1.93	2.15
first order	227	2.57	2.47
second order	139	6.74	5.36
third order	42	14.93	12.54
fourth order	2	41.35	50.70
overall	635	2.89	2.87

Table 5. Fractional Atomic Coordinates and Equivalent Isotropic Displacement Parameters[a] (Å²) for $Sr_{1.2872}NiO_3$ (Incommensurable (3+1)D Option)

	x	y	z	B_{eq}	τ
Sr	${}^1/_3$	0	${}^1/_4$	1.11(2)	
Ni1	0	0	0	0.87(4)	
Ni3a	0.0628(3)	0.0628	0	0.49(4)[b]	0.61(4)
Ni3b	0	0	0.107(8)	0.49[b]	0.28(3)
Ni3b′	0	0	−0.066(10)	0.49[b]	0.11
O	0.1553(2)	0.1553	${}^1/_2$	1.65(5)	

[a] $B_{eq} = (8\pi^2/3)\sum_i\sum_j U^{ij} a_i^* a_j^* \mathbf{a}_i \mathbf{a}_j$. [b] B_{iso}.

Commensurate (3+1)D Option. The incommensurateness of the structure was suggested by the irrational component of the wave vector (vide supra). To check this aperiodic character of the structure, a commensurate superspace group analysis was tested. Notice that this is possible since the intensity calculated from commensurate structure factors is not equal to that calculated from incommensurate structure factor.[17] For incommensurately modulated structure $\bar{x}_4$ can take all possible values between 0.0 and 1.0 (mod 1). On the contrary, for commensurately modulated structure $\bar{x}_4$ is limited to a finite number of values. From the $R\bar{3}m(00\gamma)0s$ superspace group it is possible to calculate all possible 3D space groups, assuming a general commensurate wave vector $\mathbf{q} = (m/n)\mathbf{c}^*$.[18] The various possibilities are summarized in Table 7. For $Sr_{1.2872}NiO_3$ the γ component of the modulation vector can be approximated by the 9/14 rational ratio; therefore, the appropriate 3D space groups are $R\bar{3}c$ or $R3c$. Since our 3D refinement of the structure could be carried out with the centrosymmetric space group (vide supra), we tested the commensurateness of the structure by setting $t = 0$ ($R\bar{3}c$ 3D space group).

For a commensurate modulated structure, the modulation functions are completely determined by a finite Fourier expansion.[19] Besides, a description by either modulation functions or a 3D supercell should be equivalent since it implies the same number of independent parameters.[20] For the commensurate approximation of $Sr_{1.2872}NiO_3$, the Fourier expansion harmonics are limited to four, three, and zero for Sr and Ni1; O; and Ni3a, Ni3b, and Ni3b′, respectively. However, since the satellite average intensity vanishes with their order, the Fourier expansions can be reduced. Indeed, a refinement series with displacive Fourier amplitude waves up to the fourth order for Sr and Ni1 and to the second order for O and DWF waves up to the fourth order for Sr and Ni1 and to the first order for O converged to a residue factor of 4.14% for only 47 variables, to be compared with the similar $R = 3.96\%$ value (but for 59 parameters) in the supercell description before the introduction of Gram−Charlier nonharmonic third-order tensor coefficients. The addition of more

(16) Becker, P. J.; Coppens, P. *Acta Crystallogr. A* **1974**, *30*, 129.
(17) Perez-Mato, J. M.; Madaragia, G.; Tello, M. J. *Phys. Rev. B* **1987**, *30*, 1534.
(18) Yamamoto, A.; Nakazawa, H. *Acta Crystallogr. A* **1982**, *38*, 79.
(19) Janner, A.; Janssen, T. *Physica A* **1979**, *99*, 47.
(20) Perez-Mato, J. M. In *Superspace description of commensurately structures and quasicrystals*; World Scientific Publishers: Singapore, 1991; p 117.

Table 6. Atomic Positional and DWF Modulation Coefficients[a] for $Sr_{1.2872}NiO_3$ (Incommensurable (3+1)D Option)

Ni1	$U^{Ni1}_{z,3} = -0.0209(10)$	$U^{Ni1}_{z,7} = -0.001(2)$	
	$U^{Ni1}_{U11,4} = -0.0029(6)$	$U^{Ni1}_{U33,4} = -0.005(2)$	
	$U^{Ni1}_{U11,8} = 0.0004(9)$	$U^{Ni1}_{U33,8} = 0.008(3)$	
Ni3a	$U^{Ni3a}_{x,1} = -0.0069(9)$	$U^{Ni3a}_{x,2} = -0.0010(2)$	$U^{Ni3a}_{z,2} = 0.026(2)$
O	$U^{O}_{x,1} = 0.0003(2)$	$U^{O}_{x,2} = -0.00155(11)$	$U^{O}_{x,3} = 0.00323(12)$
	$U^{O}_{x,4} = 0.0029(3)$		
	$U^{O}_{z,2} = 0.0812(9)$	$U^{O}_{z,3} = -0.0093(9)$	
	$U^{O}_{U11,1} = -0.0085(7)$	$U^{O}_{U11,2} = -0.0008(6)$	$U^{O}_{U11,3} = 0.0000(6)$
	$U^{O}_{U11,4} = 0.0019(8)$		
	$U^{O}_{U33,1} = -0.0103(13)$	$U^{O}_{U33,4} = 0.007(2)$	
	$U^{O}_{U12,1} = -0.0039(8)$	$U^{O}_{U12,4} = 0.0043(9)$	
	$U^{O}_{U13,1} = -0.005(5)$	$U^{O}_{U13,2} = 0.0104(7)$	$U^{O}_{U13,3} = -0.0023(8)$
	$U^{O}_{U13,4} = -0.004(5)$		
Sr	$U^{Sr}_{x,s1} = -0.00843(3)$	$U^{Sr}_{x,s2} = 0.00445(3)$	$U^{Sr}_{x,s4} = -0.001(2)$
	$U^{Sr}_{x,s5} = -0.031(2)$		
	$U^{Sr}_{z,s3} = 0.0007(5)$	$U^{Sr}_{z,s6} = -0.024(2)$	
	$U^{Sr}_{U11,s1} = 0.0061(2)$	$U^{Sr}_{U11,s2} = -0.0017(2)$	$U^{Sr}_{U11,c3} = -0.0095(3)$
	$U^{Sr}_{U11,s4} = -0.0057(5)$	$U^{Sr}_{U11,s5} = 0.0001(5)$	
	$U^{Sr}_{U33,c3} = -0.0023(4)$		
	$U^{Sr}_{U13,s1} = -0.0054(3)$	$U^{Sr}_{U13,s2} = -0.0059(2)$	$U^{Sr}_{U13,s4} = 0.0038(4)$
	$U^{Sr}_{U13,s5} = 0.0050(5)$		

[a] Modulation functions for a parameter λ of an atom ν defined in a restricted interval (cases of Ni1, Ni3a, and O) are given by

$$U^{\nu}_{\lambda}(\bar{x}_4) = \sum_{n=0}^{k} U^{\nu}_{\lambda,n}\ \mathrm{Ortho}^{\nu}_{n}(\bar{x}_4)$$

where the orthogonalized functions, obtained through a Schmidt orthogonalization routine, are given by

$$\mathrm{Ortho}^{\nu}_{i}(\bar{x}_4) = B^{\nu}_{0} + \sum_{n=1}^{k} A^{\nu}_{n} \sin(2\pi n\bar{x}_4) + \sum_{n=1}^{k} B^{\nu}_{n} \cos(2\pi n\bar{x}_4)$$

For Sr, the modulation functions are classically written as

$$U^{\nu}_{\lambda}(\bar{x}_4) = U^{\nu}{}_{\lambda,0} + \sum_{n=1}^{k} U^{\nu}_{\lambda,sn} \sin(2\pi n\bar{x}_4) + \sum_{n=1}^{k} U^{\nu}_{\lambda,cn} \cos(2\pi n\bar{x}_4)$$

Only independent coefficients are provided.

Table 7. 3D Space Groups Derived from the $R\bar{3}m(00\gamma)0s$ (3+1)D Superspace Group for q = (m/n)c*

$\gamma = m/n$	$t = 0$ mod ($^1/_2n$)	$t = \pm^1/_6n$ mod($^1/_2n$)	$t = {}^1/_4n$ mod($^1/_2n$)	otherwise
$m = 3k$, n even	$R\bar{3}c$	$R3c$	$R3c$	$R3c$
$m = 3k$, n odd	$R\bar{3}$	$R3$	$R32$	$R3$
$m = 3k \pm 1$, n even	$P\bar{3}c$	$P\bar{3}c$	$P3c$	$P3c$
$m = 3k \pm 1$, n odd	$P\bar{3}$	$P\bar{3}$	$P32$	$P3$

Table 8. Summary of the Refinement Results for $Sr_{1.2872}NiO_3$

	3D		(3+1)D	
	classic	nonharmonic	comm	incomm
no. of reflecns	635	635	635	635
no. of refined params	59	69	47	60
R/R_w (%)	3.96/3.95	2.92/3.09	4.14/4.10	2.89/2.87

waves in the refinements did not really improve the fit, contrary to what was observed for the incommensurate approach.

A summary of the refinement results obtained for the various models is given in Table 8.

3. Discussion

The hexagonal perovskite structures are commonly described through a stacking of mixed $[A_3O_9]$ and $[A_3A'O_6]$ layers and an occupation of the octahedral sites between those layers by B^{IV} elements, the A′ cation filling a trigonal prismatic site (see for instance ref 3). From known compounds, a general formula was established for the family: $A_{3n+3}A'_nB_{3+n}O_{9+6n}$, where n represents the number of adjacent $[A_3A'O_6]$ layers in the stacking sequence. From that n value, one should be able to deduce the actual succession of octahedra (Oh) and trigonal prismatic (TP) sites in the $[A'_nB_{3+n}O_{9+6n}]$ chains (e.g. $n = 1$ corresponds to −4Oh−1TP−, $n = 2$, to −3Oh−1TP−2Oh−1TP−, $n = 3$, to −2Oh−1TP−, etc.) However, with this formalism one cannot easily describe all known structures. For instance, $Sr_{14}Co_{11}O_{33}$ and $Sr_{24}Co_{19}O_{57}$[21] would require fractional values of n, $^9/_5$ and $^5/_3$, respectively! In addition, the proposed formulation is not applicable to incommensurate structures. A new general description had to be established.

We describe the hexagonal perovskite structures as composite structures with two chain subsystems: a $[(A',B)X_3]$ first chain subsystem and an [A] second chain subsystem. A projection along the c axis of $Sr_{18}(NiO_3)_{14}$, commensurate approximation of the title compound $Sr_{1.2872}NiO_3$, is presented in Figure 2. The two chain subsystems $[NiO_3]$ (A′ = B = Ni; X = O) and [Sr] (A = Sr) are easily identified in such a projection. With $\mathbf{q} = \gamma\mathbf{c}_s^*$ as the modulation wave vector, the simplest

(21) Gourdon, O.; Boucher, F.; Petricek, V.; Evain, M. *Acta Crystallogr. B*, to be published.

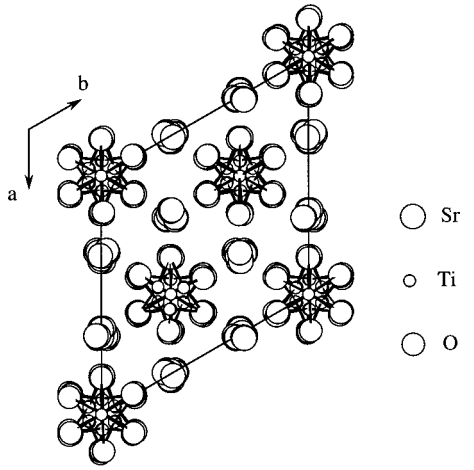

Figure 2. Projection along *c* of the $Sr_{1.2872}NiO_3$ structure (commensurate approximation).

formula that can be imagined for the hexagonal perovskites is $A_{2\gamma}(A',B)X_3$ (notice that since $\gamma = m/n$ is directly obtained from the diffraction pattern, the stoichiometry is known before starting the structure refinement). A more instructive formula can be established from our knowledge of the structure: $A_{2\gamma}A'_{2\gamma-1},B_{2(1-\gamma)}X_3$, where A′ is defined in a *t* interval of total width $2\gamma - 1$ and B in a *t* interval of total width $2(1 - \gamma)$ (vide supra). The Oh/TP site ratio is then immediately available from γ: $Oh/TP = 2(1 - \gamma)/(2\gamma - 1)$. For the title compound, one gets the formula $Sr_{1.2872}Ni_{0.2872}Ni_{0.7128}O_3$, which indicates that 28.72% of the Ni atoms are in TP sites and 71.28% are in Oh sites (a proportion close to the 2/5 commensurate approximation). The formula can be further split in the following way: $(A_2A'X_3)_{2\gamma-1}$-$(ABX_3)_{2(1-\gamma)}$. This latter formula artificially, but conveniently, separates the elements in TP sites from those in Oh sites; this will be very useful for the charge balance (vide infra). In the case of a commensurate composite structure, the γ component of **q** can be expressed as a rational fraction: $\gamma = m/n$. The formula can then be written as $(A_2A'X_3)_{2m-n}(ABX_3)_{2(n-m)}$ or equivalently as $A_{2m}A'_{2m-n}B_{2(n-m)}X_{3n}$. For the commensurate approximation of $Sr_{1.2872}NiO_3$, $\gamma = 9/14$, thus the formula $(Sr_2NiO_3)_4(SrNiO_3)_{10}$ or $Sr_{18}Ni_{14}O_{42}$. All known compounds in the family perfectly fit that scheme, as do $Sr_{14}Co_{11}O_{33}$ ($\gamma = 7/11$) and $Sr_{24}Co_{19}O_{57}$ ($\gamma = 12/19$).

To discuss the structure of $Sr_{1.2872}NiO_3$, and especially the local environment of the cations, we compare the results obtained with the 3D supercell and (3+1)D incommensurate composite models. In Figures 3 and 4 are presented the Ni−Ni, Ni−O, and Sr−Ni3a distances as a function of *t*. The values obtained for the 3D supercell model are also reported in those figures (crosses). A very good match between the two distance sets is observed. Similar agreements are observed for the other distances (Sr−O, Sr−Ni1, etc.). Notice that the use of crenel functions leads to homogeneous, readable sets of distances, contrary to what is obtained with Fourier series for occupation modulations (see for instance ref 6). In the real incommensurate composite structure, the −3Oh−1TP−2Oh−1TP− periodic succession of the ideal commensurate $[TiO_3]$ chains is only disturbed by the aperiodic insertion of −2Oh−1TP−2Oh−1TP− chain blocks. This modification is predictable since the observed γ component of **q** is larger than the rational 9/14 fraction, implying a TP/Oh site ratio greater than 2/5. However, apart from that difference and its consequence on the Ni−Ni bond alternation, the local environments in $Sr_{1.2872}NiO_3$ can be very well described from the $Sr_{18}Ni_{14}O_{42}$ commensurate approximation. Therefore, we analyze the essential features of $Sr_{1.2872}NiO_3$ by looking at the $Sr_{18}Ni_{14}O_{42}$ structural results.

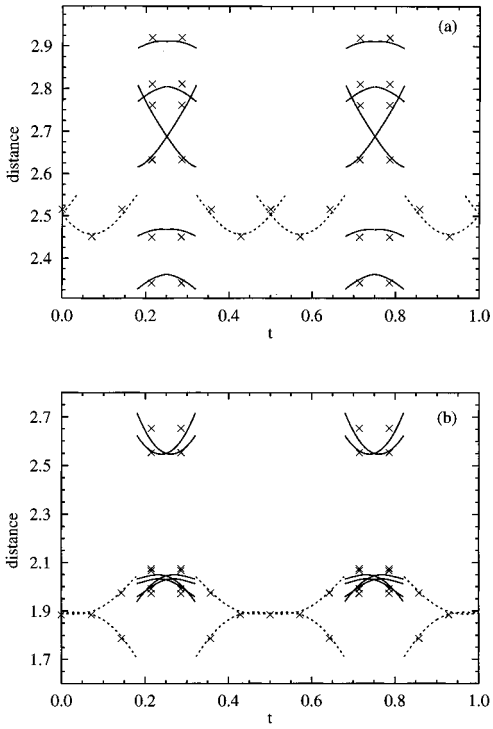

Figure 3. Ni−Ni (a) and Ni−O (b) distances (Å) as a function of the internal *t* coordinate for the (3+1)D incommensurate model. Solid and broken lines with TP and Oh Ni atoms as references, respectively. Crosses correspond to equivalent distances calculated from the 3D commensurate approximation.

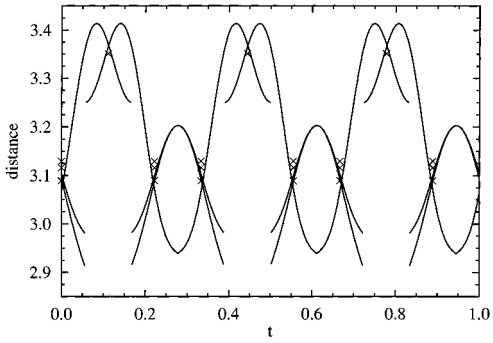

Figure 4. Sr−Ni3a distances (Å) as a function of the internal *t* coordinate for the (3+1)D incommensurate model. Crosses correspond to equivalent distances calculated from the 3D commensurate approximation.

In the $[NiO_3]$ chain, three nickel atom environments can be distinguished: octahedral for Ni1, Ni2 and Ni4, square-like for Ni3a, and trigonal prismatic for Ni3b and Ni3b′. The Ni−Ni distances between the nickel atoms of the face sharing octahedra are rather homogeneous (2.45, 2.45, and 2.52 Å, see Figure 5 and Table 9) and comparable to the distances found in Ni metal (2.49 Å). Notice that, to realize such distances, Ni2 is displaced

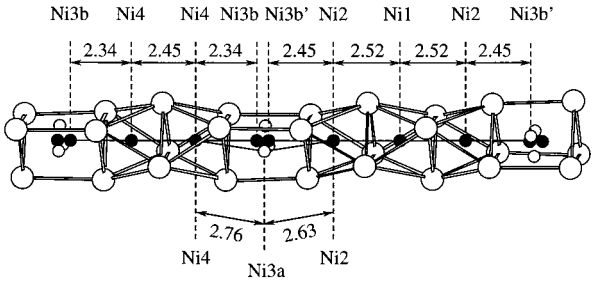

Figure 5. [NiO_3] chain in $Sr_{1.2872}NiO_3$ (3D commensurate approximation).

Table 9. Main Interatomic Distances (Å) for $Sr_{1.2872}NiO_3$ (3D Option)

Ni1−O3	1.884 (6) (6×)	Ni3a−O1	1.972 (8) (1×)
		Ni3a−O1	1.991 (8) (1×)
Ni2−O1	1.787 (6) (3×)	Ni3a−O2	2.075 (10) (1×)
Ni2−O3	1.974 (6) (3×)	Ni3a−O2	2.066 (11) (1×)
Ni4−O2	1.906 (8) (3×)	Ni3b−O2	1.964 (11) (3×)
Ni4−O4	1.916 (6) (3×)	Ni3b−O1	2.376 (12) (3×)
Ni1−Ni2	2.516 (4) (2×)	Ni3b′−O1	2.025 (9) (3×)
Ni2−Ni3b′	2.450 (11) (1×)	Ni3b′−O2	2.285 (11) (3×)
Ni2−Ni3a	2.633 (7) (3×)		
Ni2−Ni3b	2.919 (13) (1×)	Sr1−Ni3a	3.089 (3) (1×)
Ni4−Ni4	2.451 (4) (1×)	Sr1−Ni3a	3.116 (4) (1×)
Ni4−Ni3b	2.341 (13) (1×)	Sr1−Ni3a	3.129 (6) (1×)
Ni4−Ni3a	2.761 (6) (3×)	Sr1−Ni4	3.164 (3) (1×)
Ni4−Ni3b′	2.811 (10) (1×)		

from the octahedron center toward the trigonal prismatic site, which induces the shortest Ni−O distances of the structure (1.79 Å). In the TP sites, the nickel atoms are distributed over five positions: three positions in the center of the TP squarelike faces and two similar off-centered positions along the TP axis (see Figure 6). Such an arrangement was already observed for platinum in $Ba_3Pt_2O_7$,[22] although the positions were not certain given the high residual factor (8%) and the highly disordered nature of the structure. The occupation of the TP faces generates four nonequivalent Ni−O distances (2.03 Å in average) and rather short Ni3a−Sr1 contacts (3.09 Å as the shortest distance). To lengthen those latter contacts, strontium atoms are statistically displaced, thus the nonharmonic behavior observed for Sr1 in the 3D supercell approach (probability density function plots clearly show this displacement). The two last nickel positions, Ni3b and Ni3b′ on the TP axis, form three short (ca. 2 Å) and three long (ca. 2.3 Å) Ni3−O distances. The Ni3b−Ni4 and Ni3b′−Ni2 distances should be cautiously considered, given the splitting of the Ni3b atoms (Ni3b and Ni3b′) and the low site occupations (for instance, $d_{Ni3b-Ni4} = 2.34$ Å may be considered too short). The averaged Ni3a−O distance (2.03 Å) and the short Ni3b−O and Ni3b′−O distances (1.99 Å in average) suggest a +II oxidation state for the TP Ni atoms. Similarly, the Ni1−O, Ni2−O, and Ni4−O distances (1.89 Å in average) suggest a +IV oxidation state for the Oh Ni atoms.

Going back to the proposed formulation for the hexagonal perovskite compounds, $(A_2A'X_3)_{2\gamma-1}(ABX_3)_{2(1-\gamma)}$, we consider the overall charge balance. Assuming an oxidation state of +II for A and A′ and an oxidation state of IV for B, one notices that the charge balance is achieved whatever the q value since both parts,

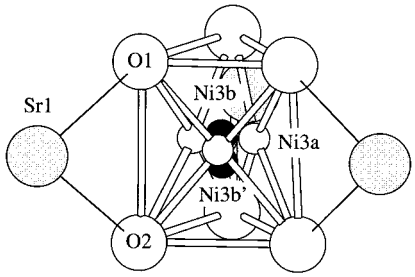

Figure 6. Distribution and environment of the trigonal prismatic nickel atoms (3D commensurate approximation).

$(A^{2+}{}_2(A')^{2+}X^{2-}{}_3)$ and $(A^{2+}B^{4+}X^{2-}{}_3)$, are neutral. This is the case for $Sr_{1.2872}NiO_3$ if two different nickel cations are considered: Ni(II) in TP sites and Ni(IV) in Oh sites, as suggested by the Ni−O distances. This is also the case for the Sr_xCoO_3 compounds already mentioned, the various compositions observed being readily understood. The situation is very similar to that of the MA_xTe_2 phases (M = Nb, Ta; A = Si, Ge; $^1/_3 \leq x \leq {}^1/_2$), where neutral [$MTe_2$] ribbons are commensurately or incommensurately incorporated into neutral [$MA_{1/2}Te_2$] layers.[23] All known hexagonal perovskite-like compounds can be charge balanced in that way, if reported nonstoichiometries are not genuine and simply the consequence of wrong structure descriptions. Notice that other charge balances with different oxidation states are possible. For instance $Sr_4Ru_2O_9$[24] can be written as $(Sr^{2+}\square_1O^{2-}{}_3)^{2-}(Sr^{2+}Ru^{5+}O^{2-}{}_3)^{1+}{}_2$. In this case, the γ component of **q** is fixed to the rational $m/n = 2/3$ value, and no other stoichiometries are expected.

4. Concluding Remarks

The stucture of the $Sr_{1.2872}NiO_3$ incommensurate composite compound has been determined. Out of the three different approaches tested, the (3+1)D incommensurate composite model with application of crenel functions yielded the best results. The 3D supercell approach gave, however, a very good structure approximation, which enabled a standard structure analysis. The essential features of the $Sr_{1.2872}NiO_3$ that were missed in the previous structure determination are (i) the incommensurate character of the structure, (ii) the splitting of the TP nickel atoms over five positions, (iii) the full occupancy of the TP sites, which induces a perfect charge balance with Ni(II) and Ni(IV) only, and (iv) the nonharmonic behavior of the disorder-affected Sr cations which, if not taken care of, seriously hampers the 3D supercell structure refinement. Such features seem to be present in all perovskite-like compounds with group 10 A′ elements (the structures being either commensurate or incommensurate). Similar features are also observed with group 9 or group 4 A′ elements, with, however, a different splitting of the TP A′ atoms.[25] The reasons for those splittings are not yet understood. To interpret the distribution, temperature dependent analyses and ab initio band structure calculations are

(22) Haradem, P. S.; Chamberland, B. L.; Katz, L.; Gleizes, A. *J. Solid State Chem.* **1977**, *21*, 217.

(23) Boucher, F.; Zhukov, V.; Evain, M. *Inorg. Chem.* **1996**, *35*, 7649.

(24) Dussarrat, C.; Fompeyrine, J.; Darriet, J. *Eur. J. Solid State Inorg. Chem.* **1995**, *32*, 3.

(25) Gourdon, O.; Cario, L.; Petricek, V.; Boucher, F.; Evain, M. *Acta Crystallogr. B*, to be published.

currently in progress. Finally, a new generic formulation is proposed for the hexagonal perovskite compounds.

Acknowledgment. V.P. and M.D. would like to thank the Grant Agency of the Czech Republic for its financial support (Grant 202/96/0085).

Supporting Information Available: Tables listing anisotropic and nonharmonic displacement parameters, final residual factors, and set functions (2 pages); tables listing structure factors (10 pages). Ordering information is given on any current masthead page.

CM9801800